Please cite this article in press as: Mukherjee et al., Multiple CheY Homologs Control Swimming Reversals and Transient Pauses in *Azospirillum brasilense*, Biophysical Journal (2019), https://doi.org/10.1016/j.bpj.2019.03.006

Biophysical *Journal*
Article

Biophysical Society

Multiple CheY Homologs Control Swimming Reversals and Transient Pauses in *Azospirillum brasilense*

Tanmoy Mukherjee,[1] Mustafa Elmas,[2] Lam Vo,[1] Vasilios Alexiades,[2] Tian Hong,[1,3] and Gladys Alexandre[1,*]
[1]Department of Biochemistry and Cellular and Molecular Biology, [2]Department of Mathematics, and [3]National Institute for Mathematical and Biological Synthesis, University of Tennessee, Knoxville, Tennessee

ABSTRACT Chemotaxis, together with motility, helps bacteria foraging in their habitat. Motile bacteria exhibit a variety of motility patterns, often controlled by chemotaxis, to promote dispersal. Motility in many bacteria is powered by a bidirectional flagellar motor. The flagellar motor has been known to briefly pause during rotation because of incomplete reversals or stator detachment. Transient pauses were previously observed in bacterial strains lacking CheY, and these events could not be explained by incomplete motor reversals or stator detachment. Here, we systematically analyzed swimming trajectories of various chemotaxis mutants of the monotrichous soil bacterium, *Azospirillum brasilense*. Like other polar flagellated bacterium, the main swimming pattern in *A. brasilense* is run and reverse. *A. brasilense* also uses run-pauses and putative run-reverse-flick-like swimming patterns, although these are rare events. *A. brasilense* mutant derivatives lacking the chemotaxis master histidine kinase, CheA4, or the central response regulator, CheY7, also showed transient pauses. Strikingly, the frequency of transient pauses increased dramatically in the absence of CheY4. Our findings collectively suggest that reversals and pauses are controlled through signaling by distinct CheY homologs, and thus are likely to be functionally important in the lifestyle of this soil organism.

INTRODUCTION

Bacteria swim using polar or lateral flagella, and chemotaxis signal transduction controls the swimming pattern in most of these motile bacteria. The most extensively studied bacterium *Escherichia coli* possesses peritrichous flagella powered by bidirectional motors, and its swimming pattern consists of straight runs interrupted by tumbles that reorient the cell in a new direction (1). When all the flagellar motors rotate counterclockwise (CCW), the rigid flagellar filaments form a bundle that propels the cell forward in a "run." When any of the flagellar motors switch rotation from CCW to clockwise (CW), the flagellar bundle is disrupted (2,3), resulting in a "tumbling" event. This swimming pattern is referred to as "run and tumble" (1).

Many motile bacteria have one or more polar flagella, including 90% of motile marine bacteria (4). For most of these polarly flagellated bacteria, the swimming pattern has not been characterized. In bacteria with polar monotrichous flagella powered by a bidirectional motor such as the alphaproteobacterium *Azospirillum brasilense*, the rotation of the flagellar motor in the CCW direction causes cells to move forward by pushing the cells, whereas CW rotation of the flagellar motor results in a backward movement (3,5). Regardless of the number of flagella, the probability of reversals in the direction of rotation of the flagellar motors is controlled by chemotaxis signaling (6). In other bacteria, chemotaxis signaling controls the probability of a unidirectional flagellar motor stopping (e.g., *Rhodobacter sphaeroides*) or slowing down (e.g., *Sinorhizobium meliloti*) (7).

In contrast to tumbles, the run and reverse swimming pattern of monotrichous flagellated bacteria could in theory lead to endless retracing of the trajectory, with reorientation in a new swimming direction depending on random thermal or Brownian motions (2,8). This represents a rather inefficient way of seeking nutrients or escaping noxious conditions by chemotaxis. The unproductive nature of this backtracking for exploration during chemotaxis led to the hypothesis that monotrichous flagellated bacteria have developed mechanism(s) to overcome this limitation (2,8). In agreement with this notion, Xie et al. (8) found that the monotrichous flagellated bacterium *Vibrio alginolyticus*

Submitted September 17, 2018, and accepted for publication March 13, 2019.

*Correspondence: galexan2@utk.edu

Editor: Joseph Falke.
https://doi.org/10.1016/j.bpj.2019.03.006

Please cite this article in press as: Mukherjee et al., Multiple CheY Homologs Control Swimming Reversals and Transient Pauses in *Azospirillum brasilense*, Biophysical Journal (2019), https://doi.org/10.1016/j.bpj.2019.03.006

could abruptly change swimming direction around an ~90° angle with a flick of its unique polar flagellum. In this bacterial species, flicking of the flagellum occurs when the cells resume a forward run after a brief backward run, causing the flagellum to buckle at the hook (8,9). This buckling of the flagellum, which depends on the swimming speed (9) and cell size (10), leads to broad reorientation of the cells at an angle centered around 90°. Evidence to date indicates that chemotaxis signaling does not control the probability of flick after a reversal event; rather, the flick was recently proposed to result from a dynamic instability on the flagellar hook and filament (9,11).

In chemotaxis, a motile organism navigates chemical gradients in the environment and directs its movement toward higher concentrations of an attractant or lower concentrations of a repellent. Motile and flagellated bacteria accomplish chemotaxis by biasing their swimming pattern to move toward favorable niches in the environment. In *E. coli* and other bacteria, chemotaxis signaling functions to alter the probability of swimming tumbles or reversals. This signaling is initiated when a stimulus is detected by chemoreceptors, causing a conformational change that ultimately alters the phosphorylation state of the associated histidine kinase CheA. Phosphorylated CheA transfers its phosphoryl group to its cognate response regulator, CheY, increasing its affinity for the flagellar motor. Binding of phosphorylated CheY to the flagellar motor triggers a switch in the direction of motor rotation, causing a tumble or swimming reversal (12). In *A. brasilense*, chemotaxis is controlled via two chemotaxis signaling pathways, named Chemotaxis (Che)1 and Che4, in which each control a distinct motility parameter (13,14). Che1 and thus CheA1 and CheY1 control transient changes in the swimming speed, (13) whereas Che4 and its histidine kinase-response regulator pair, CheA4 and CheY4, regulate the probability of swimming reversals (14). In addition to CheY1 and CheY4, the genome of *A. brasilense* encodes two additional chemotaxis systems, named Che2 and Che3, that do not control flagellar motility but other cellular functions (15) (G.A. and L. O'Neal, unpublished data), as well as two other CheYs, named CheY6 and CheY7, for which their function is not known (16). CheY6 and CheY7 have the hallmarks of chemotaxis response regulators known to affect flagellar motor activity, including conserved residues known to be essential for CheY function in *E. coli* (Fig. 1). We thus hypothesized that CheY6 and CheY7 regulate chemotaxis through effects on the probability of change in the swimming speed and/or reversals in *A. brasilense*. Here, we characterize these response regulators and identify additional features of the swimming pattern of *A. brasilense*, including pause events that are controlled by chemotaxis signaling. By characterizing the role of different CheYs in modulating the swimming pattern, we identify distinct roles for the CheY homologs that suggest, to our knowledge, novel features of the flagellar motor in this organism.

MATERIALS AND METHODS

Bacterial strains and culture conditions

The bacterial strains used in this study are listed in Table 1. Minimal medium for *A. brasilense* (MMAB) with malate (10 mM) as a carbon source and with or without nitrogen in the form of ammonium chloride (18.7 mM) (+/−N) and Che buffer were prepared as described previously (17,18). Stocks of individual strains maintained at −80°C were directly streaked on an agar-solidified nitrogen-free MMAB (−N) plate because *A. brasilense* is a diazotroph (19). A single colony from the freshly streaked plate was inoculated into 5 mL of liquid MMAB +N media with additional antibiotics when needed. The *A. brasilense* wild-type (Sp7) and mutant strains were grown at 28°C, with shaking (275 rpm). The cultures were reinoculated at least once more until the optical density $(OD)_{600}$ was 0.6 before recording swimming of the bacteria for motion-tracking analyses purposes. The cultures

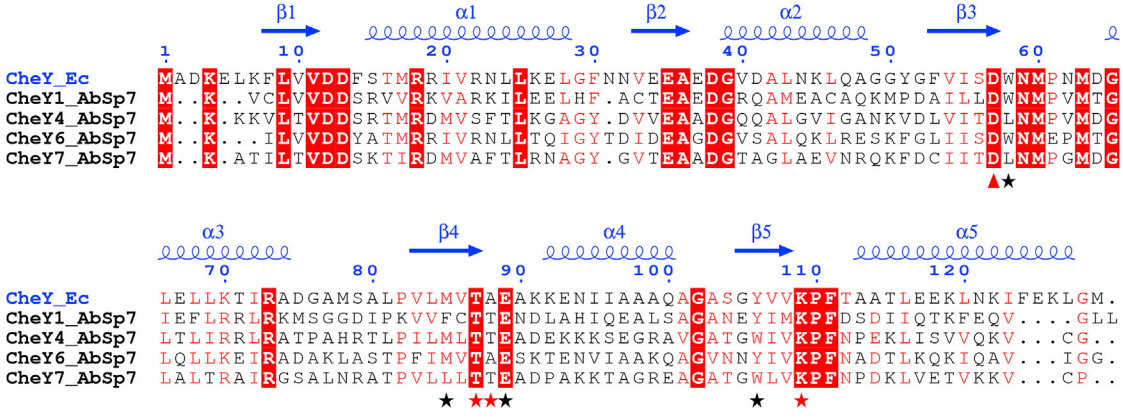

FIGURE 1 Sequence alignment for CheYs in *A. brasilense* with an *E. coli* CheY structure as a reference. The figure was generated in ESPript 3 (50) using *E. coli* CheY crystal structure (3CHY) (51). The secondary structure and residue number of the *E. coli* Che Y are presented on the top of the alignment. Red-colored background/letters depict regions of identity/similarity based on a global similarity score of 0.7. Black stars underneath the alignment depict the allosteric quartet and red stars depict the phosphorylation sensor with reference to *E. coli* CheY (52). A red, solid triangle denotes the site of phosphorylation at the conserved aspartate residue. To see this figure in color, go online.

Please cite this article in press as: Mukherjee et al., Multiple CheY Homologs Control Swimming Reversals and Transient Pauses in *Azospirillum brasilense*, Biophysical Journal (2019), https://doi.org/10.1016/j.bpj.2019.03.006

TABLE 1 Strains and Plasmids Used in This Study

Strains	Genotype	References
A. brasilense		
Wild-type	wild-type strain Sp7	ATCC 29145
ΔcheY1	*ΔcheY1*::Km (Km^r)	(20)
ΔcheY4	*ΔcheY4*::Cm (Cm^r)	(14)
ΔcheA1	*ΔcheA1*::*gusA*-Km (Km^r)	(20)
ΔcheA4	*ΔcheA4*::Gm (Gm^r)	(14)
ΔcheA1ΔcheA4	*ΔcheA1ΔcheA4*::*gusA*-Km-Gm (Km^r Gm^r)	(14)
ΔcheY7	*ΔcheY7*::Gm (Gm^r)	this work
ΔcheY6	markerless deletion that also includes first 39 bp and last 33 bp of the open reading frame of *cheY6*	this work
E. coli		
S17-1	*thi endA recA hsdR* strain with RP4-2Tc::Mu-Km::Tn7 integrated in chromosome	(45)
HB101	general cloning strain	Invitrogen
DH5-α λpir	DH5-α derivative containing *pir* gene	(46)
Plasmids		
pCR2.1	TOPO cloning vector	Invitrogen
pKNOCK	mobilized suicide plasmid for insertional deletion (pBLS63 derivative carrying RP4 *ori*T and R6K γ-*ori*, Gm^r)	(47)
pRK2013	helper plasmid for triparental mating (ColE1 replicon, Tra, Kan)	(48)
pK18mobsacB	suicide vector for gene disruption; *lacZ mob sac*B Km^r	(22)
pCRSOECheY6	pCR2.1 with SOECheY6 fragment	this work
pK18SOECheY6	pK18mobsacB with SOECheY6	this work
pCRInterCheY7	pCR2.1 with 164 bp internal fragment of *cheY7*	this work
pKNOCKInterCheY7	pKNOCK vector with internal fragment of *cheY7* cloned into the BamHI sites	this work
pRK415	broad-host-range plasmids for in *trans* complementation (RSF1010 and RK404 derivatives, Tet^r)	(49)
pRKCheY1	pRK415 with *cheY1*	(14)
pRKCheY4	pRK415 with *cheY4*	(14)
pRKCheY6	pRK415 with *cheY6*	this work
pRKCheY7	pRK415 with *cheY7*	this work

were then harvested and washed in 1 mL of Che buffer (three times at 3000 × *g*) for 3 min and resuspended in Che buffer to a final concentration of OD_{600} = 0.01–0.05 for recording. The samples were left undisturbed for at least 30 min before recording free-swimming cells to adapt. All recordings were completed within 2 h of collecting the initial cultures. Unless stated, the antibiotics were used at the following concentrations: 200 μg/mL ampicillin, 50 μg/mL carbenicillin, 25 μg/mL kanamycin (Km), 20 μg/mL gentamycin (Gm), and 20 μg/mL chloramphenicol (Cm).

Mutagenesis

Construction of mutant strains *ΔcheY1* and *ΔcheY4* were previously described (14,20) (Table 1). The strain carrying a *ΔcheY6* deletion was made using an allelic exchange method (17) as follows. A 418-bp upstream DNA sequence, including the first 39 bases of *cheY6*, was amplified using primers 1F and 1R (Table S1). Similarly, a 410-bp downstream DNA sequence, including the last 33 bases of *cheY6*, was amplified using primers 2F and 2R (Table S1). These two fragments were then fused using splicing by overlap extension PCR (21) using primers 1F and 2R and cloned into pCR2.1 resulting in pCRSOECheY6. The pCRSOECheY6 vector was then digested with *Eco*RI and ligated into the *Eco*RI-digested suicide vector pK18mobsacB (22). The resulting vector pK18SOECheY6 was transformed into *E. coli* S17-1 cells and mobilized into *A. brasilense* through biparental mating following the previously described protocol (17). To construct the *ΔcheY7* mutant strain, a 164-bp internal fragment of *cheY7* was amplified using primers Inter_CheY7_FwdBamHI and Inter_CheY7_RevBamHI (Table S1). The resulting fragment was cloned into the pCR2.1 vector to generate pCRInterCheY7. The pCRInterCheY7 vector and the suicide vector pKNOCK(Gm^r) were then digested with BamHI. The BamHI-digested internal fragment of *cheY7* was ligated into BamHI-digested pKNOCK(Gm^r) to generate pKNOCKInterCheY7. The pKNOCKInterCheY7 plasmid was then transformed into *E. coli* DH5-α λpir and mobilized into *A. brasilense* by triparental mating using *E. coli* HB101 (pRK2013) as a helper, as previously described (17). The mutations did not cause any growth defect whether the antibiotics were added or not.

Complementation assay

All primers, plasmids, and bacterial strains used in constructing complementation mutants are listed in Table S1 and Table 1. *che*Y6 was amplified with primers CheY6KpnI_CompFwd and CheY6SacI_CompFwd, and cheY7 was amplified with primers CheY7KpnI_CompFwd and

Please cite this article in press as: Mukherjee et al., Multiple CheY Homologs Control Swimming Reversals and Transient Pauses in *Azospirillum brasilense*, Biophysical Journal (2019), https://doi.org/10.1016/j.bpj.2019.03.006

CheY7SacI_ CompRev. The amplified *che*Y6 and *che*Y7 were fused with plasmid pRK415 via the restriction digest/ligation method, as described above, to make plasmids pRKCheY6 and pRKCheY7, respectively. pRKCheY6 and pRKCheY7 were then transformed into *E. coli* S17-1 and mobilized into *Δche*Y6 and *Δche*Y7 by biparental mating. Control strains with empty pRK415 plasmids were constructed in similar fashion.

For the swim assay, complementation strains were streaked from glycerol stock stored at −80°C on an MMAB −N agar plate. A single colony from each strain was inoculated in MMAB +N medium and grown until the OD_{600} was 0.6–0.8. The culture was then reinoculated in fresh MMAB +N medium until the OD_{600} was 0.3–0.4. 5 μL of the culture was inoculated into 0.2% agar nutrient broth (13 g/L) with appropriate antibiotics. The plate was incubated at 28°C for 36 h, and the ring diameter was measured.

For recording the swimming video, complementation strains were grown in MMAB +N overnight until dense. The following day, the cultures were then reinoculated with fresh MMAB +N medium until the OD_{600} was 0.6. Cells were collected by centrifugation at 3000 × *g* and washed with Che buffer. The washed cultures were left for at least 30 min, like the condition described above. The behaviors of swimming cells were recorded using the same setup used for recording swimming trajectories described below.

Video tracking of free-swimming cells

All recordings were done using a Concavity Microscope Slide from Thermo Fisher Scientific (category no. 1518006; Waltham, MA). These slides have a concave depression with 5 (bottom)-18 mm (top) diameter well and are 0.6–0.8 mm deep. A 10-μL drop of culture in Che buffer was placed in the middle of the depression well and covered with a coverslip (Corning cover glass; category no. 2975-223; Corning, NY). A minimum of three separate 10-μL drops of culture were used for recording from the same-day culture. The experiment was repeated on two more separate days. The coverslip, in addition to the necessary contrast, also provided a setting in which there was little or no perturbation due to air flow. The recording was done using a Nikon E200 upright microscope equipped with a 20× phase contrast objective (Plan Fluor extra-long working distance; ×20; numerical aperture 0.45; Nikon, Minato, Tokyo, Japan). The microscope was focused such that the focal plane was at least 300–400 μm away from the surface. All recordings of free-swimming cells were captured using a Leica MC120 HD digital camera (Leica Microsystems, Buffalo Grove, IL) at 30 fps at a 1920 × 1080-px resolution.

Image processing and cell tracking

Video recordings were processed using custom software written in MATLAB (The MathWorks, Natick, MA) to extract and analyze individual cell trajectories. A bandpass filter using the Gaussian average for each nearby pixel was applied to all frames to reduce the random noise from individual pixels. A background image was then constructed by calculating the mean pixel intensities of the frames over the image sequence and subtracted from each image in the image stack to exclude nonmoving cells. A 3 × 3 median filter was then applied to the background-free frames. In each frame, cells were segmented by an automatically selected intensity threshold, which was dependent on the brightest pixels in the frame. The locations of all cells in each frame were determined by calculating the centroid (center of mass) of the brightest pixels in frames. Cells were linked from frame to frame by identifying the nearest neighbor in the later frame for each cell in the prior frame. A MATLAB version of the particle tracking algorithm was used to link the positions of cells in each frame to reconstruct trajectories in time and space (23).

Cell tethering assay

Overnight cultures in minimal medium were reinoculated into fresh medium and grown to an OD_{600} of 0.6. Cells were collected by centrifugation at 3000 × *g* and washed with Che buffer three times before being resuspended in Che buffer for 30 min for allowing cells to adjust. An *A. brasilense* antipolar flagellin antisera (25) prepared at a 1/1000 dilution in phosphate buffer saline was spotted on a cleaned coverslip and air dried. Washed cells were aliquoted on the surface of a glass slide chamber made with three layers of tape, as described in (24). The coverslips coated with the dried antisera were placed on top of the cell chamber, ensuring that the liquid touched the coverslip. The behavior of tethered cells attached was recorded using the same setup used for recording swimming trajectories described above. The videos obtained were further processed and analyzed using MATLAB as described in (26).

Postprocessing

Only trajectories with a tracked duration greater than 2 s were considered for final analysis. Trajectories with an average speed of less than 15 μm/s were also discarded to avoid including dead or slow-moving cells in the analysis. Trajectories of colliding cells were discarded manually. Cells tend to change swimming direction at the beginning and end of each trajectory because this is the most common way to enter or leave the focal plane. Thus, we eliminated the first and last five frames of each recorded track to avoid overestimating the reversal frequency. The tracks with the highest median curvature were removed because these tracks performed reversal for a very long time. The trajectories were smoothed with three-frames running average, and all the statistics were applied to these smoothed trajectories.

We recorded 1360 swimming tracks for wild-type *A. brasilense* in a quasi-two-dimensional setup, and after initial processing as mentioned above, 1317 tracks were selected for further analysis (Table S2). A similar screening was performed for the tracks of the various chemotaxis mutants of *A. brasilense*, and an average number of at least 1000 processed trajectories were used for each strain for final analysis (Table S2). We selected only 361 tracks for the *ΔcheA1ΔcheA4* mutant because these cells tend to stick to each other under the conditions of this experiment and thus lose motility rapidly. We also calculated the distribution of trajectory time duration for each strain and found very similar profiles across all the strains used in this study (Fig. S1). From the cell trajectories, we computed multiple aspects of cell movement, including the average run speed, maximal speed, minimal speed, average run time, acceleration, reversal frequency, average angle of reversal, pause frequency, average pause time, and mean-square displacement of bacteria. Turning events were identified by rapid changes in speed and/or direction of motion as discussed in Theves et al. (27).

Cell speed was measured as the scalar quantity representing the distance moved between consecutive frames, divided by the time elapsed in between. Given the position $(x(t), y(t))$ of a cell at time t, its speed at time t is calculated as

$$v(t) = \frac{\sqrt{(x(t) - x(t - \Delta t))^2 + (y(t) - y(t - \Delta t))^2}}{\Delta t},$$

where Δt is the time interval between two consecutive frames. $x(t)$ is the x-coordinate of the cell and $y(t)$ is the y-coordinate of the cell.

We defined angular velocity as

$$\omega(t) = \frac{\theta(t) - \theta(t - \Delta t)}{\Delta t},$$

where $\theta(t) = \arctan(\Delta y/\Delta x)$, $\Delta y(t) = y(t + \Delta t) - y(t)$, and $\Delta x(t) = x(t + \Delta t) - x(t)$.

Turn and pause detection

To detect the events in which the cells make abrupt turns and/or pauses, we used the method described previously by Theves et al. (27) and Masson

Please cite this article in press as: Mukherjee et al., Multiple CheY Homologs Control Swimming Reversals and Transient Pauses in *Azospirillum brasilense*, Biophysical Journal (2019), https://doi.org/10.1016/j.bpj.2019.03.006

et al. (28). To identify angular velocity changes, we first detected local maxima in the absolute value of the angular velocity. The time when a local maximum was achieved is denoted by t_{max}. The location of the two closest local minima immediately before and after t_{max} are denoted respectively by t_1 and t_2. If the total change in direction over the interval $[t_1, t_2]$ was sufficiently larger than a threshold, which depends on the rotational diffusivity ($|\Delta\theta| > 7\sqrt{D_r(t_2 - t_1)}$, where $D_r = 0.1\ rad^2/s$, we considered the bacterium was undergoing directional change during the time interval around t_{max} such that the angular speed $\omega(t)$ satisfied the condition

$$|\omega(t_{max})| - |\omega(t)| \leq 0.7\ \Delta\omega,$$

with $\Delta\omega = \max|(\omega(t_{max})| - |\omega(t_1)|, |\omega(t_{max})| - |\omega(t_2)|)$

To identify abrupt changes in speed, we first detected local minima of the instantaneous velocity, where the time when a local minimum was achieved is indicated by t_{min}. The location of two closest local maxima immediately before and after t_{min} are denoted, respectively, by t_1 and t_2. We computed the relative change in speed as

$$\frac{\Delta v}{v(t_{\min})},$$

where

$$\Delta v = \max(v(t_1) - v(t_{min}), v(t_2) - v(t_{min})).$$

If the relative change of velocity was sufficiently large,

$$\frac{\Delta v}{v(t_{\min})} > 2,$$

we considered the bacterium was undergoing a change in speed (defined as "pausing events") during the time interval around t_{min} such that

$$v(t) \leq v(t_{min}) + 0.2\ \Delta v.$$

The threshold parameters for pauses and reversals are similar to previous studies (27,28). We confirmed the validity of these parameters by visual inspection of the trajectories (see Fig. 2 for examples). We adjusted the arbitrary constant in the second part of the equation above (changed between 0.2 and 2) to identify the two different types of pauses identified by the algorithm and confirmed them by manually checking all tracks before subsequent analysis.

Based on the bimodal distributions (centered at 0° and 180°) of the directional changes during the pauses, we partitioned the pausing events into transient pauses (<90°) and reversals (≥90°). As such, the reversal events exhibit both an abrupt decrease in speed and a significant change of directions.

RESULTS

Distinct reversal and pause swimming patterns in *A. brasilense*

To characterize the swimming patterns of *A. brasilense*, we first examined the distributions of the angles during the turning events (defined based on an abrupt increase in angular velocity and significant directional change (see Materials and Methods for details)) in wild-type strain Sp7 (Fig. 2 A). The distribution of the turning angles is centered at 180°, with a long tail extended below 90°. This pattern suggests that the majority of turning events are "reversals" during which the bacteria completely switched their swimming directions. One example of such events is shown in Fig. 2 B. In this example, bacteria made three abrupt turns (Fig. 2 B, *yellow track segments*) with angles close to 180°. Together with the straight motion before the turning events, these events constitute the "run-reverse" swimming patterns that were well characterized before (29). We surmise they correspond to reversals of the direction of rotation of the polar flagellar motor from CCW to CW, which were observed in other bacteria and in *A. brasilense* (5,29). Unlike bacteria that have a three-step swimming pattern of run-reverse-flick and have a broad peak centered around 90° (8), we did not observe a distinct population of turning events with angles centered around 90° (Fig. 2 A). Nonetheless, we found that a minor population of the turning events exhibit the "flick-like" pattern (Fig. 2 C) (run-reverse-flick), and it is possible that flicking events with angles distributed broadly around 90° occurred (Fig. 2 A). This suggests the possibility that *A. brasilense* may use flicking-like motion as a secondary swimming strategy.

We next characterized the events in which the bacteria have abrupt decreases in swimming speed (see the Materials and Methods for details). The turning angles during these events have a remarkable bimodal distribution (Fig. 2 D). We observed a significant number of events with turning angles distributed around each of the modes at 180° and 0°. Based on this bimodal distribution, we classified these events into two categories: those with turning angles less than 90° are defined as "transient pauses" (Fig. 2 D, *blue population* (see example in Fig. 2 E)), and the rest are defined as reversals (Fig. 2 D, *red population*) because they are strongly correlated with the abrupt turning events (Fig. 2 B, *yellow segments* and *red dots*; Fig. 2 F, Pearson correlation coefficient: 0.89; p-value < 0.0001). For those transient pauses, *A. brasilense* decreased its swimming speed abruptly during a swimming run and then resumed the swim in the same direction (Fig. 2 D, run-pause, with pauses labeled as *red dots*). Note that we use reversals to refer to the events with both detected sharp decrease in speed and significant directional change (Fig. 2 D, *red population*) for convenience, but it is possible to use the term to describe the abrupt turning events (Fig. 2 A) because of their strong correlation (Fig. 2 F). This strong correlation between reversal frequency and abrupt turns is also true for all chemotaxis mutants used in this study (Fig. S2 and next section). Hence, all of our conclusions are not sensitive to this choice of terminology.

The examples shown in Fig. 2, B and E suggest that the transient pauses and the reversals are distinct swimming patterns. We asked whether this distinction is generally valid in the tracked cells. We found that the frequencies of observing the transient pauses and observing the reversals are not correlated among the tracks (Fig. 2 G). Notably, there are significant numbers of tracks that have either transient pauses only or reversals only (Fig. 2 G, *data points on*

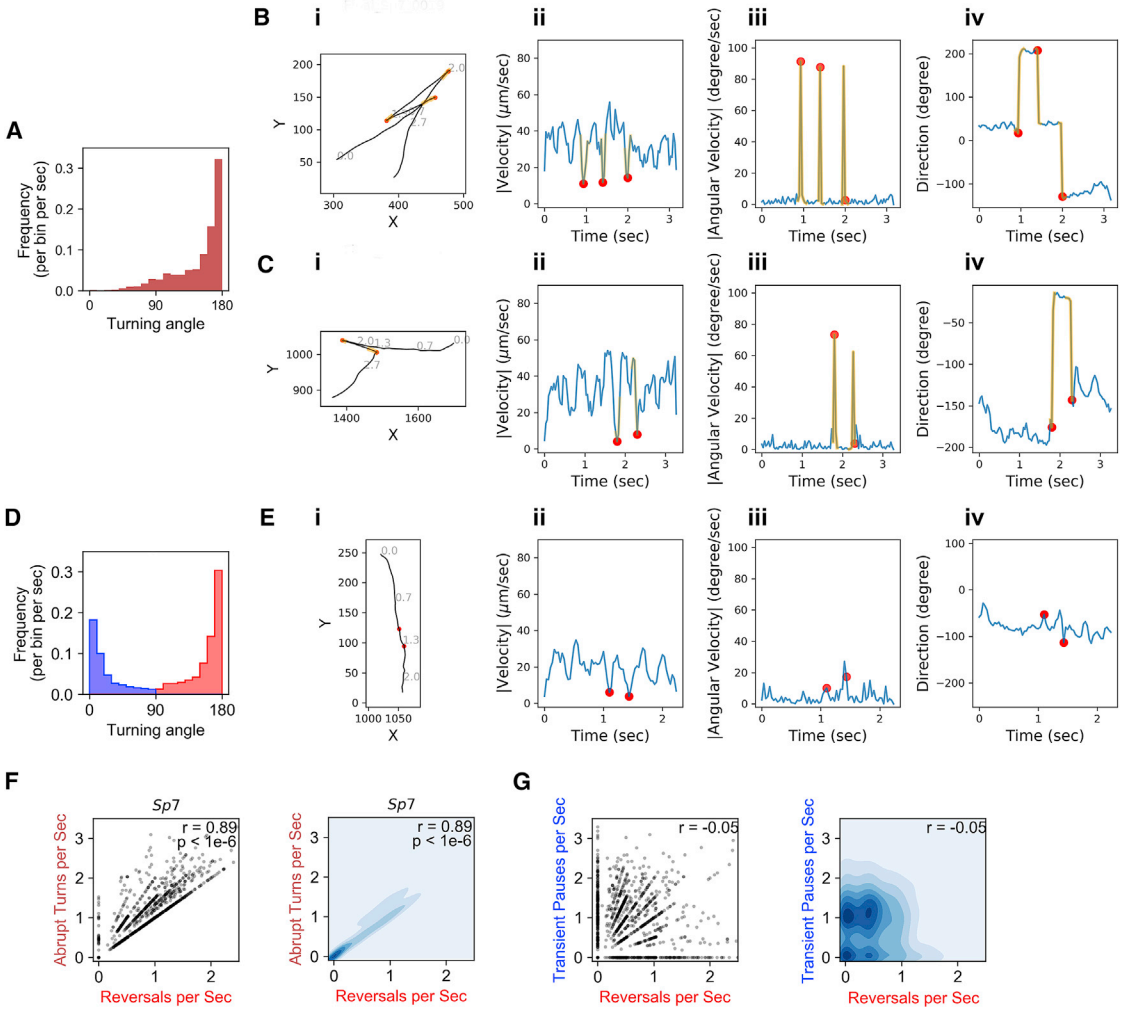

FIGURE 2 Quantification and presentation of different aspects of the swimming patterns in wild-type *A. brasilense*. (*A*) The distribution of turning angles during swimming in wild-type *A. brasilense* is shown. (*B*) *i*) A run-reverse swimming pattern as seen in wild-type *A. brasilense* is shown. (*C*) *i*) A run-reverse-flick-like event as seen during swimming of wild-type *A. brasilense* is shown. (*D*) The distribution of events with transient pause and reversals as classified based on turning angle threshold. (*B*, *C*, and *E*) *ii*) The instantaneous speed, *iii*) angular velocity, and *iv*) direction of travel for the same trajectory are shown in separate horizontal panels. (*E*) A typical trajectory with two consecutive transient pauses is shown. (*F*) A scatter plot and kernel density plot showing the correlation of abrupt turns/s versus reversals/s is shown. (*G*) A scatter plot and kernel density plot showing the correlation of transient pauses/s versus reversals/s. The yellow color in (*B*) and (*C*) represents the frames involved in the turning event, whereas the red dot represents a transient pause. The blue shading in the right panels of (*F*) and (*G*) indicate density of the events, with darker blue meaning more events. To see this figure in color, go online.

the x or y axis). The apparent lack of strict association between pauses and reversals indicates that the transient pauses may not merely correspond to incomplete motor reversal events that were described earlier (30), and they might be controlled by mechanisms distinct from those controlling the reversals.

In summary, we found that free-swimming *A. brasilense* cells display distinct run-reverse and run-pause patterns, and we also observed infrequent run-reverse-flick events in these cells. We next performed a detailed analysis on these remarkably diverse swimming patterns, in particular, on the transient pauses that were not well characterized in previous studies.

Signaling through CheA4 and CheY4 controls the frequency of transient pauses

To examine the molecular machinery that controls the swimming patterns of *A. brasilense*, we used strains in which chemotaxis genes encoding for CheA and CheY homologs were mutated. The genome of *A. brasilense* encodes two additional CheYs, named CheY6 and CheY7, in addition to CheY1 and CheY4 that we characterized before (16). CheY2, CheY3, and CheY5 are noncanonical chemotaxis response regulators that lack key residues for interaction with flagellar motors and are thus unlikely to function in chemotaxis (Fig. 1). Therefore, we only

Please cite this article in press as: Mukherjee et al., Multiple CheY Homologs Control Swimming Reversals and Transient Pauses in *Azospirillum brasilense*, Biophysical Journal (2019), https://doi.org/10.1016/j.bpj.2019.03.006

considered CheY6 and CheY7 in this study. Previously, we found that there are two changes associated with chemotaxis in *A. brasilense*: transient changes in the swimming speed and in the reversal frequency, with CheA and CheY homologs controlling these distinct outputs previously identified (13,14): CheA1 and CheY1 control increases in swimming speed and CheA4 and CheY4 control the probability of swimming reversals. The motility defects caused by mutation of these chemotaxis genes were restored by expressing a parental copy of these genes in the corresponding mutant, indicating the mutations are nonpolar and that they directly cause the chemotaxis defect observed (13,14,20). Therefore, we analyzed the swimming speed, swimming reversals, and transient pauses in these strains. All strains analyzed swam at a lower speed relative to the wild-type strain (Fig. S3, A and B). As expected from their role in controlling transient increases in speed, the *ΔcheA1* and *ΔcheY1* mutant strains had the lowest swimming speed, which was also similar to that of the *ΔcheY6* and *ΔcheY7* mutants. The speed reduction was far more modest, yet significant, for the *ΔcheA4* and *ΔcheY4* mutant strains. The *ΔcheA1ΔcheA4* mutant strain swam at a speed slower than that of the *ΔcheA1* mutant, and the speed of the *ΔcheA1ΔcheA4* strain seemed to result from the combined effect of mutating *cheA1* and *cheA4* (Fig. S3, A and B). This additive phenotype suggests that the effect of CheA1-CheY1 signaling on swimming speed, which is currently unknown, is distinct from that of CheA4-CheY4. Next, we analyzed the frequency of swimming reversals and transient pauses in these strains (Fig. 3). Compared to the wild-type strain Sp7, the *ΔcheA1*, *ΔcheA1ΔcheA4*, *ΔcheY1*, *ΔcheY4*, and *ΔcheY6* had a reduced probability of reversals, and the *ΔcheA4* and *ΔcheY7* were null and swam in straight runs. These results are consistent with phenotypes reported for *ΔcheA4* (14) and further suggest that CheY7, the mutation of which phenocopies the *ΔcheA4* mutation, functions with CheA4 as the main regulator of the swimming reversal frequency. The chemotaxis and motility defects caused by mutation in genes coding for CheY6 and CheY7 were partially restored by expressing a parental copy in *trans* from a plasmid, probably because of the lack of control of protein expression levels using this plasmid system (Fig. S4). We have obtained similar results with other mutations in *A. brasilense* in the past (13–15). Despite these limitations, the results are consistent with the mutations not being polar. Similar to the effect on speed, the probability of reversals of the *ΔcheA1ΔcheA4* mutant represented an average of the probability of reversals of the *ΔcheA1* and the *ΔcheA4* single mutants, suggesting each corresponding protein affects the cell's reversal frequency through distinct mechanisms, a hypothesis proposed earlier by us (20). Next, we determined the frequency of transient pauses in these mutants relative to the wild type. The average frequency of transient pauses was unaffected in the *Δche*A1 mutant and significantly decreased in the *ΔcheA4*, *ΔcheA1ΔcheA4*, *ΔcheY1*, *ΔcheY6*, and *ΔcheY7* mutant strains, with *ΔcheA4* and *ΔcheY7* having a similarly reduced probability of transient pauses. Lack of CheY1 function had the least effect on the pause frequency, followed by CheY6 and CheY7, which had the most significant effect. Unexpectedly, the probability of transient pauses was increased in the *ΔcheY4* mutant strain relative to the wild type. Consistent with these observations, the reversal frequency did not correlate with transient pause frequency among the strains (Fig. 4) or among the tracks in each strain (Fig. 5). These data are consistent with CheY7 being the major chemotaxis response regulator affecting the flagellar motor in *A. brasilense*. We used a cell tethering assay to validate the frequency of pauses and reversals in the wild type, the *ΔcheY4* and *ΔcheY7* mutant strains because these represent drastically distinct phenotypes (Videos S1, S2, and S3). These analyses corroborated the findings from tracking free-swimming cells: CheY4 functions to suppress pauses, whereas CheY7 increases the pauses, and both of these also affect, albeit to a different degree, the probability of swimming reversals. Given the role of chemotaxis signaling in the frequency of transient pauses, we also investigated if the change in the duration of both reversal and transient pauses has any effect on turning angles. In *A. brasilense*, the duration of the pause events did not correlate with the turning angle in the wild type or any of the nonchemotactic mutants (Fig. 6, A

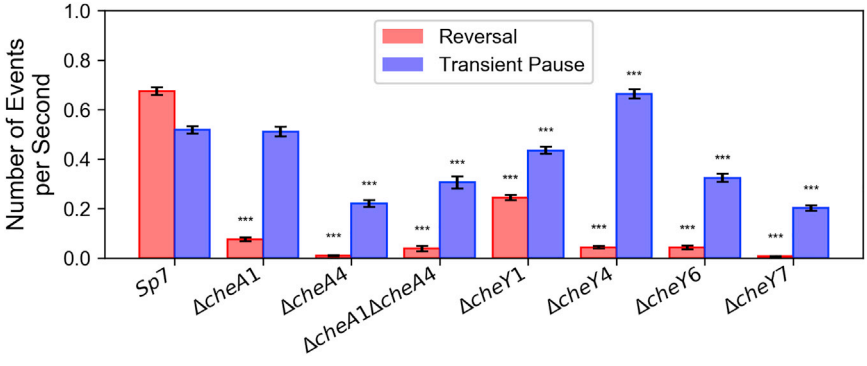

FIGURE 3 Frequency of transient pauses (*blue*) and reversals (*red*) for each of the chemotaxis mutants tested in this study. Mean frequencies for each strain were calculated and error bars represents the standard error of means. The number of tracks analyzed for each strain are presented in Table S1. A pairwise comparison was done for each strain with wild-type (Sp7) for statistical significance separately for reversal frequency and transient pause frequency. Those marked by (***) represent statistically significant differences at $p < 0.001$ level (Student's *t*-test). To see this figure in color, go online.

Please cite this article in press as: Mukherjee et al., Multiple CheY Homologs Control Swimming Reversals and Transient Pauses in *Azospirillum brasilense*, Biophysical Journal (2019), https://doi.org/10.1016/j.bpj.2019.03.006

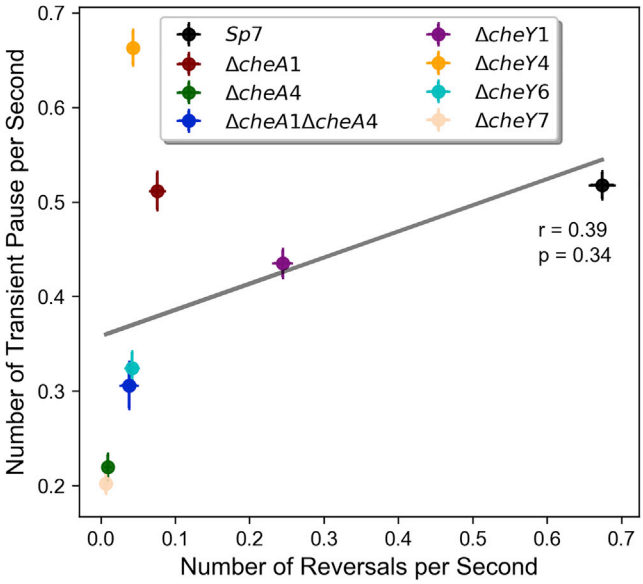

FIGURE 4 Frequency of transient pauses do not correlate with reversals frequency. The correlation of transient pauses/s versus reversals/s for all the chemotaxis strains used in this study is shown. A weak and nonsignificant correlation is seen with a Pearson correlation coefficient of 0.39 (p-value = 0.34). To see this figure in color, go online.

and B). These data also suggest that 1) multiple CheY homologs contribute to regulating the probability of transient pauses, 2) CheA1 has no role in controlling the frequency of transient pauses, and 3) CheA4, probably through CheY7, plays a major role in the reversal of motor rotation. Although these data indicate that a lower reversal frequency is associated with a lower probability of transient pauses, this relationship is not exclusive, as illustrated with the phenotype of the *ΔcheY4* mutant. Combined, our results suggest that control of pauses and control of reversals are distinct behaviors that depend on signaling through different CheY homologs in *A. brasilense*.

DISCUSSION

In this work, we identified three patterns of free-swimming *A. brasilense* cells: run-reverse, run-pause, and run-reverse-flick. These different patterns of swimming allow a population of swimming *A. brasilense* cells to sample its environment by changing direction at angles spanning 0°–180°. Although most directional changes were observed around 180° angles under the conditions used here, this behavior may increase competitiveness in the soil environment. Indeed, the soil is a spatially and temporally heterogeneous structure comprised of aggregates of varying sizes and pore spaces that create a range of chemical gradients (31). The ability of a motile cell to explore the surroundings using different swimming patterns that produce a broad range of turning angles could be advantageous in the spatially and temporally heterogenous environment of the soil.

The run-reverse swimming pattern is ubiquitous in polarly flagellated bacteria (4,32). The run-reverse-flick pattern was first identified in the marine bacteria *Vibrio aliginolyticus* and *Pseudoalteromonas haloplanktis*, both of which have a single polar flagellum that rotates rapidly, imparting high swimming speeds of up to ~70 μm/s (9). Son et al. (9) increased the Na^+ ion concentration in the culture medium, which increased the swimming speed of the sodium-driven motor of *V. aliginolyticus* and measured the number of cells that flicked. These experiments led them to conclude that the flicking probability increases with speeds over 35 μm/s (9). Motile soil-dwelling bacteria that have been studied thus far swim slower than marine bacteria because of their proton-driven flagellar motor

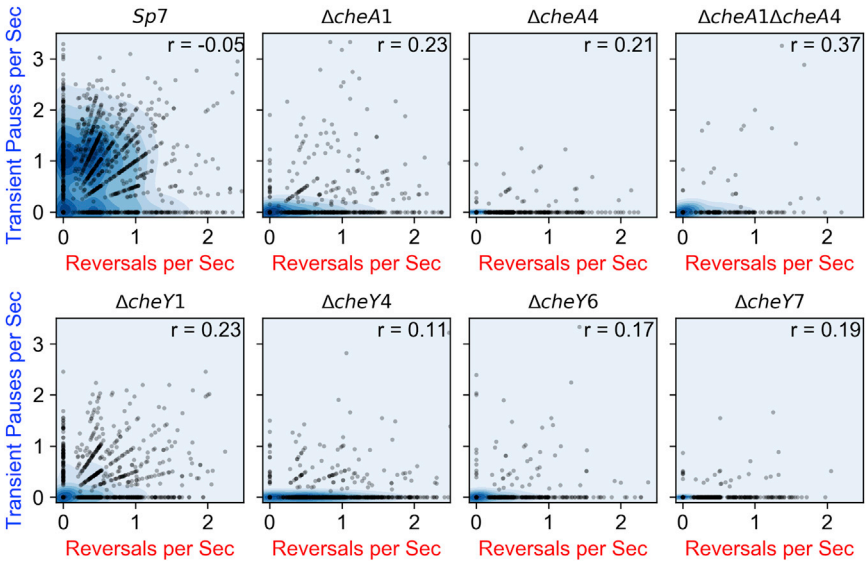

FIGURE 5 Correlation of transient pauses/s versus reversals/s for all the chemotaxis strains used in this study shown individually. Scatter plots and kernel density plots show distributions of pause/reversal frequencies for all tracks of each strain. Correlation between transient pauses/s versus reversals/s for varies from no relationship ($r = -0.05$) in wild-type (Sp7) to a weak positive linear relationship in *ΔcheA1ΔcheA4* ($r = 0.37$). The blue shading indicates the density of the events, with darker blue meaning more events. To see this figure in color, go online.

Please cite this article in press as: Mukherjee et al., Multiple CheY Homologs Control Swimming Reversals and Transient Pauses in *Azospirillum brasilense*, Biophysical Journal (2019), https://doi.org/10.1016/j.bpj.2019.03.006

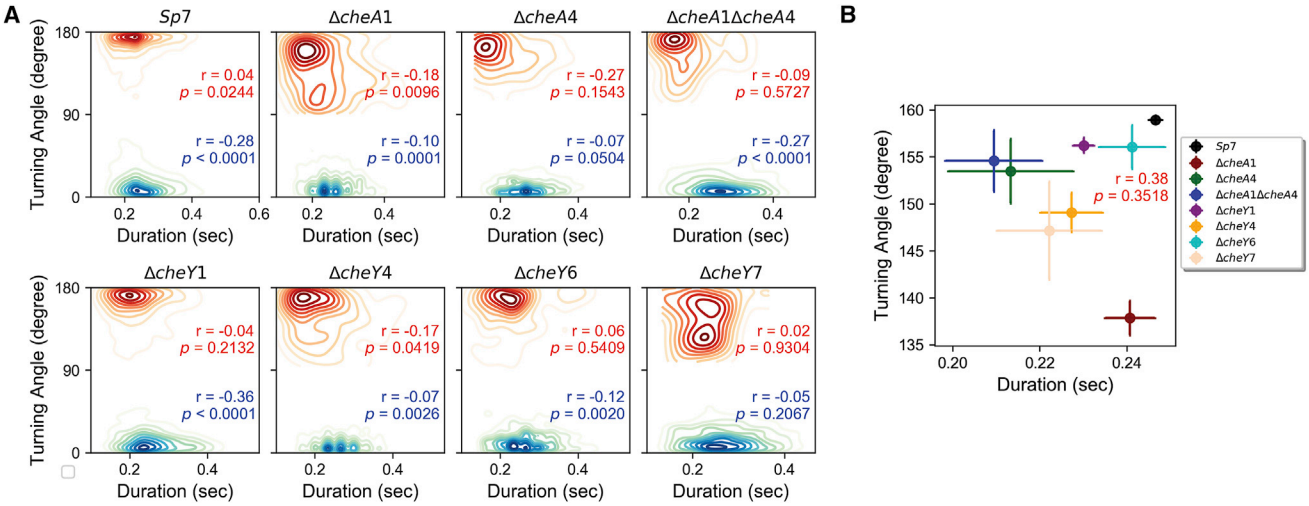

FIGURE 6 (*A*) Kernel density plots showing the distribution of turning angle does not correlate with duration of transient pauses or reversals. The correlation of turning angle versus the duration of transient pause and reversals for all the chemotaxis strains used in this study shown individually with *p*-values for each strain is shown. The Pearson correlation coefficient (*r*) is denoted in red for reversals and blue for transient pauses in each panel. The *p*-value for each of the strains is provided in their respective panels. (*B*) The correlation of turning angles and durations of transient pauses for all strains used in this study is shown. A Pearson correlation coefficient of 0.38 (*p*-value = 0.3518) shows weak positive correlation between turning angles and transient pause duration. To see this figure in color, go online.

(33). Except for the bacterium *Pseudomonas oryzihabitans*, flicks have not been conclusively identified in any other soil-dwelling motile bacteria (34). The average speed of motile *A. brasilense* cells is 30 μm/s with a rather broad distribution around this average value (Fig. S3 A) (14). Given this distribution, it is likely that a minor fraction of motile *A. brasilense* cells swim at speeds greater than 30 μm/s and that could result in an increased probability of flicking with higher speeds. Additional analysis, including higher resolution microscopy, will be required to conclusively establish whether flicks do occur in *A. brasilense*.

Our results indicate that chemotaxis protein CheA4 controls transient pauses and all reversals, most likely by signaling through CheY7, which displays a similar phenotype. These observations would suggest that transient pauses correspond to incomplete reversals in the direction of rotation of the flagellar motor, which was also observed in *E. coli* (35,36). These pause events were associated with changes in the direction of rotation of the flagellar motor during a tumble because nonchemotactic mutants, including a mutant lacking CheY, that are unable to tumble no longer pause (36,37). In *E. coli*, these transient pauses were later observed experimentally (30,36). Transient pauses during swimming were also observed in three *Pseudomonas* species (*P. putida*, *P. fluorescens*, and *P. aeruginosa*), and the dependence on motor reversal was found to be similar to that of *E. coli* (24,38,39). Transient stator detachment was proposed as one possible mechanism for swimming pauses in *E. coli* (40). Recently, tethering experiments carried out at high angular and temporal resolution to characterize flagellar motor rotation in *E. coli* revealed that a cell lacking CheY paused with a frequency of 10 pauses/s with each pause event averaging 5 ms. The pause duration range varied from 5 to 33 ms in 90% of the pauses analyzed, but these were not accompanied by any evidence of stator displacement (41). These observations led the authors to hypothesize that most pause events in *E. coli* are caused by a mechanism other than stator displacement or incomplete reversals (41). The timescale resolution for the pauses detected in our study is 33 ms and greater. Therefore, we cannot draw any conclusions on the existence of any molecular event occurring at shorter timescales.

In contrast to *E. coli* and *Pseudomonas* species, the transient pauses observed in *A. brasilense* were not strictly associated with changes in the direction of flagellar motor rotation because a strain lacking CheY4 had a low frequency of reversals but an increased frequency of transient pauses. This suggests that transient pauses can be regulated independently of swimming reversals and that signaling through CheY4 is a major regulator of flagellar motor pauses. The phenotype of the CheY4 is unexpected for several reasons. First, CheA4 and CheY4 are produced from the *che*4 cluster and function together to control reversals (14). Unlike the control of swimming reversals, CheY4 has a divergent role on the control of the transient pauses, suggesting that either CheY4 binds the flagellar switch complex differently than any other CheY, which is unlikely given its role in reversals and the overall amino acid sequence conservation, or that CheY4 and perhaps all or only some of the other CheY homologs regulate the pause frequency through interaction with an additional protein or protein(s). Our previous work has provided evidence of complex signaling during chemotaxis in *A. brasilense* with behavioral responses

Please cite this article in press as: Mukherjee et al., Multiple CheY Homologs Control Swimming Reversals and Transient Pauses in *Azospirillum brasilense*, Biophysical Journal (2019), https://doi.org/10.1016/j.bpj.2019.03.006

depending on signaling from Che1 and Che4 (13,14,20). Additional evidence suggests that signals from Che1 and Che4 are integrated via an unknown mechanism at the level of chemotaxis receptors (42,43). Whereas CheA1 and CheY1 were shown to directly regulate transient increases in swimming speed, CheA4 and CheY4 as well as additional CheY homologs were shown to regulate the probability of swimming reversals (14). Results obtained here are fully consistent with these previous observations because we identified a role for both CheY6 and CheY7 in controlling swimming reversals, with CheY7 having a major role under the conditions of the experiments. The requirement for multiple chemotaxis proteins and CheY homologs for controlling the swimming pattern is not unique to *A. brasilense*. Chemotaxis in *R. sphaeroides* depends on signaling from CheOp1, CheOp2, and CheOp3 as well as multiple CheY homologs that are required in different combinations to control the swimming pattern by affecting flagellar motor activity (44). Together, these data suggest that the direction of rotation as well as the pauses exhibited by the polar flagellar motor of *A. brasilense* are regulated and thus, likely have a functional role. Given the reversal and pause phenotype of a strain lacking CheY4 that contrasts from those lacking CheY6 or CheY7, we hypothesize that the pause events involve unidentified additional proteins that may have features allowing them to interact with CheY homologs and structural components of the flagellar motor.

SUPPORTING MATERIAL

Supporting Material can be found online at https://doi.org/10.1016/j.bpj.2019.03.006.

AUTHOR CONTRIBUTIONS

T.M. and G.A. designed research. T.M. and L.V. performed research. M.E. and T.H. wrote codes in MATLAB and Python, respectively. T.M., M.E., T.H., and G.A. analyzed data. T.M., T.H., and G.A. wrote the article.

ACKNOWLEDGMENTS

This research is supported by National Science Foundation (grant NSF-MCB 1330344 to V.A. and G.A.). Any opinions, findings, conclusions, or recommendations expressed in this material are those of the authors and do not necessarily reflect the views of the National Science Foundation.

REFERENCES

1. Berg, H. C., and D. A. Brown. 1972. Chemotaxis in Escherichia coli analysed by three-dimensional tracking. *Nature.* 239:500–504.
2. Goto, T., K. Nakata, …, Y. Magariyama. 2005. A fluid-dynamic interpretation of the asymmetric motion of singly flagellated bacteria swimming close to a boundary. *Biophys. J.* 89:3771–3779.
3. Elgeti, J., R. G. Winkler, and G. Gompper. 2015. Physics of microswimmers–single particle motion and collective behavior: a review. *Rep. Prog. Phys.* 78:056601.
4. Leifson, E., B. J. Cosenza, …, R. C. Cleverdon. 1964. Motile marine bacteria. I. Techniques, ecology, and general characteristics. *J. Bacteriol.* 87:652–666.
5. Zhulin, I. B., and J. P. Armitage. 1993. Motility, chemokinesis, and methylation-independent chemotaxis in *Azospirillum brasilense*. *J. Bacteriol.* 175:952–958.
6. Berg, H. C. 2000. Motile behavior of bacteria. *Phys. Today.* 53:24–29.
7. Attmannspacher, U., B. Scharf, and R. Schmitt. 2005. Control of speed modulation (chemokinesis) in the unidirectional rotary motor of Sinorhizobium meliloti. *Mol. Microbiol.* 56:708–718.
8. Xie, L., T. Altindal, …, X. L. Wu. 2011. From the cover: bacterial flagellum as a propeller and as a rudder for efficient chemotaxis. *Proc. Natl. Acad. Sci. USA.* 108:2246–2251.
9. Son, K., J. S. Guasto, and R. Stocker. 2013. Bacteria can exploit a flagellar buckling instability to change direction. *Nat. Phys.* 9:494–498.
10. Taute, K. M., S. Gude, …, T. S. Shimizu. 2015. High-throughput 3D tracking of bacteria on a standard phase contrast microscope. *Nat. Commun.* 6:8776.
11. Jabbarzadeh, M., and H. C. Fu. 2018. Dynamic instability in the hook-flagellum system that triggers bacterial flicks. *Phys. Rev. E.* 97:012402.
12. Wadhams, G. H., and J. P. Armitage. 2004. Making sense of it all: bacterial chemotaxis. *Nat. Rev. Mol. Cell Biol.* 5:1024–1037.
13. Bible, A., M. H. Russell, and G. Alexandre. 2012. The Azospirillum brasilense Che1 chemotaxis pathway controls swimming velocity, which affects transient cell-to-cell clumping. *J. Bacteriol.* 194:3343–3355.
14. Mukherjee, T., D. Kumar, …, G. Alexandre. 2016. Azospirillum brasilense chemotaxis depends on two signaling pathways regulating distinct motility parameters. *J. Bacteriol.* 198:1764–1772.
15. Bible, A. N., G. K. Khalsa-Moyers, …, G. Alexandre. 2015. Metabolic adaptations of Azospirillum brasilense to oxygen stress by cell-to-cell clumping and flocculation. *Appl. Environ. Microbiol.* 81:8346–8357.
16. Wisniewski-Dyé, F., K. Borziak, …, I. B. Zhulin. 2011. *Azospirillum* genomes reveal transition of bacteria from aquatic to terrestrial environments. *PLoS Genet.* 7:e1002430.
17. Vanstockem, M., K. Michiels, …, A. P. Van Gool. 1987. Transposon mutagenesis of Azospirillum brasilense and Azospirillum lipoferum: physical analysis of Tn5 and Tn5-Mob insertion mutants. *Appl. Environ. Microbiol.* 53:410–415.
18. Gullett, J., L. O'Neal, …, G. Alexandre. 2017. Azospirillum brasilense: laboratory maintenance and genetic manipulation. *Curr. Protoc. Microbiol.* 47:3E.2.1–3E.2.17.
19. Tarrand, J. J., N. R. Krieg, and J. Döbereiner. 1978. A taxonomic study of the Spirillum lipoferum group, with descriptions of a new genus, Azospirillum gen. nov. and two species, Azospirillum lipoferum (Beijerinck) comb. nov. and Azospirillum brasilense sp. nov. *Can. J. Microbiol.* 24:967–980.
20. Bible, A. N., B. B. Stephens, …, G. Alexandre. 2008. Function of a chemotaxis-like signal transduction pathway in modulating motility, cell clumping, and cell length in the alphaproteobacterium *Azospirillum brasilense*. *J. Bacteriol.* 190:6365–6375.
21. Horton, R. M., H. D. Hunt, …, L. R. Pease. 1989. Engineering hybrid genes without the use of restriction enzymes: gene splicing by overlap extension. *Gene.* 77:61–68.
22. Schäfer, A., A. Tauch, …, A. Pühler. 1994. Small mobilizable multipurpose cloning vectors derived from the Escherichia coli plasmids pK18 and pK19: selection of defined deletions in the chromosome of Corynebacterium glutamicum. *Gene.* 145:69–73.
23. Crocker, J. C., and D. G. Grier. 1996. Methods of digital video microscopy for colloidal studies. *J. Colloid Interface Sci.* 179:298–310.
24. Qian, C., C. C. Wong, …, K. H. Chiam. 2013. Bacterial tethering analysis reveals a "run-reverse-turn" mechanism for Pseudomonas species motility. *Appl. Environ. Microbiol.* 79:4734–4743.
25. Moens, S., M. Schloter, and J. Vanderleyden. 1996. Expression of the structural gene, laf1, encoding the flagellin of the lateral flagella in Azospirillum brasilense Sp7. *J. Bacteriol.* 178:5017–5019.

26. Lele, P. P., T. Roland, …, H. C. Berg. 2016. The flagellar motor of Caulobacter crescentus generates more torque when a cell swims backward. *Nat. Phys.* 12:175–178.
27. Theves, M., J. Taktikos, …, C. Beta. 2013. A bacterial swimmer with two alternating speeds of propagation. *Biophys. J.* 105:1915–1924.
28. Masson, J. B., G. Voisinne, …, M. Vergassola. 2012. Noninvasive inference of the molecular chemotactic response using bacterial trajectories. *Proc. Natl. Acad. Sci. USA.* 109:1802–1807.
29. Taylor, B. L., and D. E. Koshland, Jr. 1974. Reversal of flagellar rotation in monotrichous and peritrichous bacteria: generation of changes in direction. *J. Bacteriol.* 119:640–642.
30. Bai, F., R. W. Branch, …, R. M. Berry. 2010. Conformational spread as a mechanism for cooperativity in the bacterial flagellar switch. *Science.* 327:685–689.
31. Vos, M., A. B. Wolf, …, G. A. Kowalchuk. 2013. Micro-scale determinants of bacterial diversity in soil. *FEMS Microbiol. Rev.* 37:936–954.
32. Johansen, J. E., J. Pinhassi, …, Å. Hagström. 2002. Variability in motility characteristics among marine bacteria. *Aquat. Microb. Ecol.* 28:229–237.
33. Oster, G., and H. Wang. 2003. Rotary protein motors. *Trends Cell Biol.* 13:114–121.
34. Lanfranconi, M. P., H. M. Alvarez, and C. A. Studdert. 2003. A strain isolated from gas oil-contaminated soil displays chemotaxis towards gas oil and hexadecane. *Environ. Microbiol.* 5:1002–1008.
35. Lapidus, I. R., M. Welch, and M. Eisenbach. 1988. Pausing of flagellar rotation is a component of bacterial motility and chemotaxis. *J. Bacteriol.* 170:3627–3632.
36. Eisenbach, M., A. Wolf, …, O. Asher. 1990. Pausing, switching and speed fluctuation of the bacterial flagellar motor and their relation to motility and chemotaxis. *J. Mol. Biol.* 211:551–563.
37. Berg, H. C. 2003. The rotary motor of bacterial flagella. *Annu. Rev. Biochem.* 72:19–54.
38. Cai, Q., Z. Li, …, V. D. Gordon. 2016. Singly flagellated Pseudomonas aeruginosa chemotaxes efficiently by unbiased motor regulation. *MBio.* 7:e00013.
39. Hintsche, M., V. Waljor, …, C. Beta. 2017. A polar bundle of flagella can drive bacterial swimming by pushing, pulling, or coiling around the cell body. *Sci. Rep.* 7:16771.
40. Yuan, J., and H. C. Berg. 2008. Resurrection of the flagellar rotary motor near zero load. *Proc. Natl. Acad. Sci. USA.* 105:1182–1185.
41. Nord, A. L., F. Pedaci, and R. M. Berry. 2016. Transient pauses of the bacterial flagellar motor at low load. *New J. Phy.* 18:115002.
42. Stephens, B. B., S. N. Loar, and G. Alexandre. 2006. Role of CheB and CheR in the complex chemotactic and aerotactic pathway of Azospirillum brasilense. *J. Bacteriol.* 188:4759–4768.
43. Russell, M. H., A. N. Bible, …, G. Alexandre. 2013. Integration of the second messenger c-di-GMP into the chemotactic signaling pathway. *MBio.* 4:e00001–e00013.
44. Porter, S. L., G. H. Wadhams, …, J. P. Armitage. 2006. The CheYs of Rhodobacter sphaeroides. *J. Biol. Chem.* 281:32694–32704.
45. Simon, R., U. Priefer, and A. Puhler. 1983. A broad host range mobilization system for in vivo genetic engineering: transposon mutagenesis in gram negative bacteria. *Nat. Biotechnol.* 1:784–791.
46. Platt, R., C. Drescher, …, G. J. Phillips. 2000. Genetic system for reversible integration of DNA constructs and lacZ gene fusions into the Escherichia coli chromosome. *Plasmid.* 43:12–23.
47. Alexeyev, M. F. 1999. The pKNOCK series of broad-host-range mobilizable suicide vectors for gene knockout and targeted DNA insertion into the chromosome of gram-negative bacteria. *Biotechniques.* 26:824–826, 828.
48. Figurski, D. H., and D. R. Helinski. 1979. Replication of an origin-containing derivative of plasmid RK2 dependent on a plasmid function provided in trans. *Proc. Natl. Acad. Sci. USA.* 76:1648–1652.
49. Keen, N. T., S. Tamaki, …, D. Trollinger. 1988. Improved broad-host-range plasmids for DNA cloning in gram-negative bacteria. *Gene.* 70:191–197.
50. Robert, X., and P. Gouet. 2014. Deciphering key features in protein structures with the new ENDscript server. *Nucleic Acids Res.* 42:W320–W324.
51. Volz, K., and P. Matsumura. 1991. Crystal structure of Escherichia coli CheY refined at 1.7-A resolution. *J. Biol. Chem.* 266:15511–15519.
52. McDonald, L. R., M. J. Whitley, …, A. L. Lee. 2013. Colocalization of fast and slow timescale dynamics in the allosteric signaling protein CheY. *J. Mol. Biol.* 425:2372–2381.